BJRS
BRAZILIAN JOURNAL OF RADIATION SCIENCES

doi.org/10.15392/2319-0612.2026.2938
Braz. J. Radiat. Sci., Rio de Janeiro
2026, 14(1) | 01-19 | e2938
Editor: Prof. Dr. Bernardo Maranhão Dantas
Editor: Prof. Dr. Alfredo Lopes Ferreira Filho
Submitted: 2025-05-14
Accepted: 2025-11-27

Original Article

Application of Optically Stimulated Luminescence Dosimeters in the Evaluation of the Dose Map Software in Interventional Radiology

Santos[a*], E.S.; Nersissian[b], D.Y.; Yoshimura[b], E.M.

[a] Faculdade de Medicina da Universidade de São Paulo, São Paulo, Brasil.
[b] Departamento de Física Nuclear, Instituto de Física da Universidade de São Paulo, São Paulo, Brasil

*Correspondence: e.souza4@hc.fm.usp.br

Abstract: Interventional radiology is widely employed; however, the complexity and duration of certain procedures may result in significant radiation exposure to patients. This study presents a comparison between a commercial computational dose mapping method used in interventional radiology, Dose Map, and optically stimulated luminescence dosimetry using a matrix built with these dosimeters. The dosimetric material was obtained from a roll of Landauer Luxel® tape and calibrated on a GE® Innova 4100 IQ angiography system, using an ionization chamber as a reference. The calibration yielded a linear relationship between the readout signal and the air kerma. Experiments were conducted using homogeneous poly(methyl methacrylate) phantoms, as well as clinical monitoring of patients. The maximum deviation between kerma values measured by the dosimeters and those estimated by Dose Map was 14%. The comparison among the dosimeter matrix, radiochromic film, and Dose Map demonstrated good geometric agreement in both phantom studies and patient monitoring. These results confirm the applicability of Dose Map for real-time dose monitoring, contributing to improved patient safety in interventional radiology.

Keywords: interventional radiology, entrance skin kerma, peak skin dose, OSL dosimetry.

BJRS
BRAZILIAN JOURNAL OF RADIATION SCIENCES

doi.org/10.15392/2319-0612.2026.2938
Braz. J. Radiat. Sci., Rio de Janeiro
2026, 14(1) | 01-19 | e2938
Editor: Prof. Dr. Bernardo Maranhão Dantas
Editor: Prof. Dr. Alfredo Lopes Ferreira Filho
Submitted: 2025-05-14
Accepted: 2025-11-27

Uso de Dosímetros por Luminescência Opticamente Estimulada na Avaliação do Software Dose Map na Radiologia Intervencionista

Resumo: A radiologia intervencionista possui diversas aplicações, no entanto, a complexidade e a duração de certos procedimentos podem resultar em exposição significativa à radiação para os pacientes. Este estudo apresenta uma comparação entre um método comercial de mapa de doses utilizado em radiologia intervencionista, o Dose Map, e dosimetria por luminescência opticamente estimulada, utilizando uma matriz construída com esses dosímetros. O material dosimétrico foi obtido a partir de um rolo de fita Landauer Luxel® e calibrado em um angiógrafo GE® Innova 4100 IQ, utilizando uma câmara de ionização como referência. A calibração resultou em uma relação linear entre o sinal de leitura e o kerma no ar. Foram realizados experimentos com objetos simuladores homogêneos de polimetilmetacrilato, bem como um acompanhamento clínico de pacientes. A máxima diferença entre os valores de kerma medidos pelos dosímetros e os estimados pelo Dose Map foi de 14%. A comparação entre a matriz de dosímetros, o filme radiocrômico e o Dose Map demonstrou boa concordância geométrica, tanto nos estudos com objetos simuladores quanto no acompanhamento de pacientes. Os resultados confirmam a aplicabilidade do Dose Map para o monitoramento da distribuição de doses na pele em tempo real, contribuindo para a segurança dos pacientes na radiologia intervencionista.

Palavras-chave: radiologia intervencionista, kerma no ar de referência, dose na pele, dosimetria OSL.

SBPR

1. INTRODUCTION

Interventional radiology (IR) is a medical specialty that performs minimally invasive image-guided procedures, offering several advantages over the conventional interventions, such as a low risk of infection and reduced patient recovery time [1]. However, due to the complexity and duration of some of these procedures, doses to patient may reach values of several gray (Gy). These levels of exposure may result in tissue reactions, such as hair loss, erythema, and, in extreme cases, necrosis [2]. Therefore, the implementation of effective strategies to track radiation dose and to optimize procedures is necessary to reduce risks and ensure patient safety [3]. There are different methods that can be utilized to assess the patient dose, ranging from the use of softwares associated with the imaging system to independent dosimetric methods.

As an attempt to simplify dose monitoring in interventional radiology, the International Electrotechnical Commission (IEC) defined a patient entrance reference point (PERP) as a point located 15 cm below the isocenter, toward the X-ray tube for fixed C-arm equipments [4]. PERP is used as the position where the reference air kerma ($K_{a,r}$) is presented. Additionally, the Radiation Dose Structured Report (RDSR) [5] is a standardized document to systematize the information related to the dose delivered to the patient during the procedure. With its use, it is possible to monitor the irradiation parameters, as well as the patient dose information.

Dose Map (DM) is a computational method available in some equipment from General Electric® (GE), which also helps in the patient dose evaluation. It creates a map of dose distribution on a surface representative of the patient, using system settings and geometry, and taking into account the estimates of table attenuation and backscatter [6]. This map can be monitored in real time during the procedure and can be recorded in the institution's Picture Archiving and Communication System (PACS). DM generates an image

that displays the distribution of the patient's entrance skin dose (ESD) in a grayscale, making it possible to identify the region of peak skin dose (PSD) [6]. In addition to mapping the dose distribution, DM provides information of the $K_{a,r}$ of the entire procedure, which is an important parameter for patient dose estimates.

An independent dosimetric method is the use of radiochromic films, which are made of polymeric materials that change color when irradiated. The intensity of this color is related to the radiation dose received at a specific location. They can be used for dosimetry in both radiotherapy [7–9] and interventional procedures [10–12]. One of the advantages of these films is the immediate visualization of the qualitative dose distribution, without the need for subsequent chemical processing. Additionally, with proper calibration, dose values can be estimated using a appropriate scanner to acquire color intensities.

Other independent dosimetric technique uses materials that demonstrate optically stimulated luminescence (OSL) as detectors. This method is based on the measurement of the light emitted by materials that trap electrons at a metastable energy level due to irradiation [13]. An advantage of optically stimulated luminescence dosimeters (OSLDs) is that a portion of the signal can be preserved after reading. This is achieved through pulsed optically stimulated luminescence (POSL) [13], a technique that enables the acquisition of the light signal using short stimulation times. This allows the luminescent material to be read more than once, by simply applying a signal loss correction factor to a subsequent reading result [14].

This study intends to compare the maps generated by DM software with those constructed from an OSLD's matrix data, and to evaluate the $K_{a,r}$ value presented by the software with the measured one. Additionally, radiochromic films are used for a qualitative evaluation of these dose maps.

2. MATERIALS AND METHODS

2.1. OSLDs calibration

The OSLD material used in this study was obtained from a roll of Landauer Luxel® tape, whose dosimetric material is carbon-doped aluminum oxide (Al_2O_3:C) in powder form, placed between plastic strips. The samples were cut in sizes of 20.0 × 0.5 cm², and ten of these strips were used for air kerma calibration. Before any irradiation of the OSLDs, they were subjected to a signal bleaching process for at least 8 hours, under four Digilight ATEC fluorescent white lamps, each with a power of 55 W.

The irradiations were performed using a GE® Innova 4100 IQ angiography system, located at the IR sector of the Instituto de Radiologia (INRAD) at the Hospital das Clínicas, Faculdade de Medicina, Universidade de São Paulo (HCFMUSP). The "*Vias Biliares*" (biliary tract) clinical protocol was used, with a tube voltage of 84 kV, an additional 0.3 mm copper filter and a field size of 40 x 40 cm². The calibration curve was constructed with four air kerma values at the PERP, ranging from 300 to 1600 mGy, measured using a Radcal® ionization chamber (IC) with a sensitive volume of 60 cm³, duly calibrated at a secondary standard laboratory. For each kerma value, two OSLDs strips were irradiated. Additionally, a pair of non-irradiated OSLDs strips was separated for background signal (BG) measurement.

An experimental diagram is presented in Figure 1. Eight poly(methyl methacrylate) (PMMA) blocks of 30 × 30 cm² were used as attenuating material, totaling a thickness of 21.3 cm. The lower block, in contact with the table, has a U-shaped cut to accommodate the IC and the OSLDs during irradiations. The distances were set so that the IC and OSLDs were positioned at the same height as the PERP, 57 cm from the X-ray tube focal spot.

The OSLDs readings were performed using a pulsed light reader (POSLI), located at the Laboratório do Grupo de Dosimetria das Radiações do Instituto de Física da Universidade de São Paulo, developed in-house [14].

Figure 1: Experimental diagram showing the PMMA blocks (in blue) and the IC (black) on the table of a C-arm IR equipment

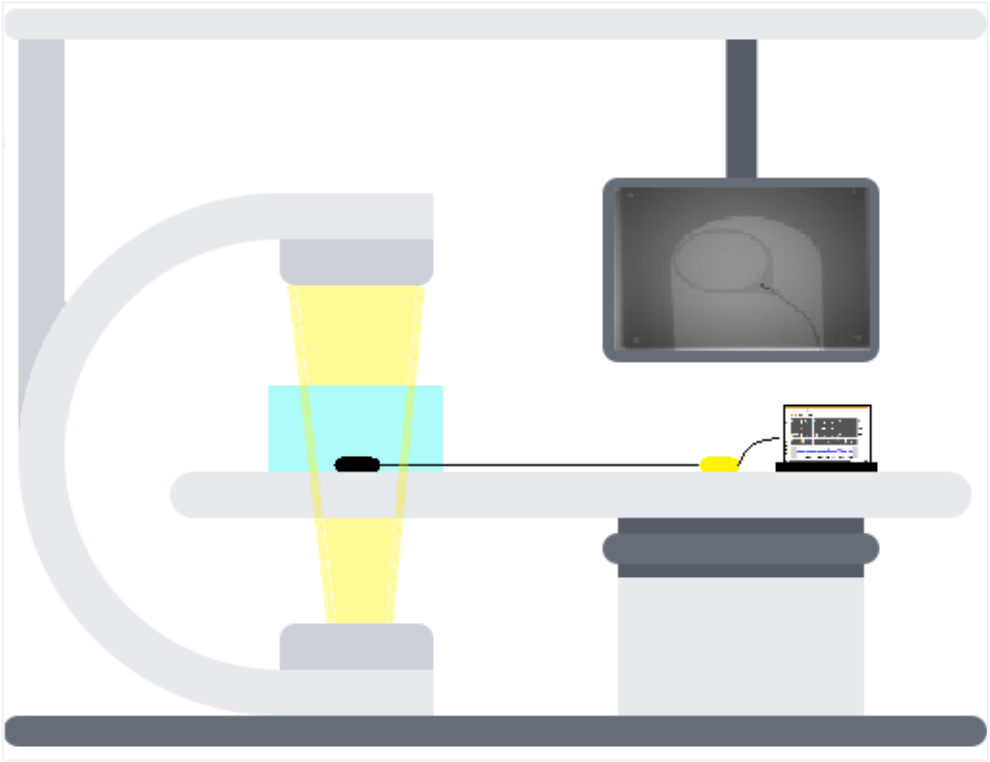

Source: the author

As result of each OSLD strip reading, POSLI reader software generates a data file with two columns: the first containing the position in millimeters, and the second the corresponding OSL signal, expressed in counts. For the analysis of the data obtained from each OSLD strip, the average signal value was calculated along the entire length of the strip, as the field size and positioning guarantee the dose homogeinity. Additionally, the average of the two strips irradiated with the same air kerma value was calculated. The Type A uncertainties associated with these data were calculated and are presented with $k = 1$ (68% confidence level).

Both Type A and Type B uncertainties were considered in air kerma measurements performed with IC. Type B uncertainties include the calibration factor of the IC, the accuracy specified in the equipment manual, and the resolution of the displayed reading value. All uncertainties were propagated and are presented with $k = 1$.

2.2. Comparison of the $K_{a,r}$ from the Dose Map and OSLDs

To compare the $K_{a,r}$ value presented in DM with the air kerma measured using OSLDs, an experimental setup similar to the one shown in Figure 1 was assembled. Ten OSLDs strips were used, irradiated in pairs with four different air kerma values, and one additional non-irradiated pair was separated for BG measurement. The strips were placed between the examination table and the PMMA attenuator, positioned at a height equivalent to PERP, and irradiated with a 40 × 40 cm² field size. For each pair of irradiated OSLDs strips, a different patient was registered in the equipment software to generate a unique DM and RDSR, which could be compared to the corresponding OSLDs readings. To compare the $K_{a,r}$ values obtained with DM to the air kerma measured by the OSLDs, the accuracy deviation was calculated using Equation 1, where K_{OSL} is the air kerma measured by the OSLD and K_{DM} is the $K_{a,r}$ value reported by DM.

$$Accuracy\ Deviation\ (\%) = \frac{K_{OSL} - K_{DM}}{K_{OSL}} \times 100 \quad (1)$$

DM presents the reference air kerma, $K_{a,r}$, and the uncertainty for these values were obtained from the RDSR, wich reports an uncertainty of 35%. Due to the measurement setup using PMMA blocks, the OSLDs are affected by backscattered radiation from the PMMA. Considering this, after converting the OSL signal into air kerma, the resulting values were divided by a backscatter factor of 1.63, based on the reference tables from IAEA TRS 457 [15]. Thus, the air kerma values obtained from the OSLDs were corrected to represent air kerma free in air (K_a), making them more comparable to $K_{a,r}$.

2.3. Dose mapping with Phantoms

DM also presents the distribution map of the patient's ESD, displayed in grayscale, where the brighter areas indicate higher dose values, as shown in Figure 2. Based on the $K_{a,r}$ value for each irradiation, the software calculates the ESD distribution using Equation 2. In this equation, $d_{Ka,r}$ and d_{KPE} represent the distances from the X-ray tube focal spot to PERP and to the patient's entrance surface, respectively. *SCF* is the geometric correction factor,

while *Att* and *Diff* are the attenuation and diffusion correction factors from the table and the mattress, respectively. *BSF* refers to the backscatter factor [6].

$$ESD = K_{a,r} \times \frac{d_{Ka,r}^2}{d_{KPE}^2} \times SCF \times Att \times Diff \times BSF \quad (2)$$

Figure 2: Dose Map software interface displayed on the computer screen. On the left side of the image, the $K_{a,r}$ value is shown, and on the right side, the ESD distribution calculated using Equation 2

Source: Screenshot of the Dose Map software

Twenty-seven OSLDs strips were used to construct the matrices intended for DM evaluation. In total, three square matrices measuring 22 cm on each side were assembled, each with nine OSLDs strips arranged according to the geometry shown in Figure 3. The OSLDs were labeled C1 to C9 in the craniocaudal direction. This labeling provided a reference for the construction of dose maps from the reading data.

Figure 3: Diagram of the matrix used for evaluating the dose mapping method of the Dose Map software. The position references shown correspond to a patient in the supine position on the examination table. All dose mapping images presented in this study follow this orientation.

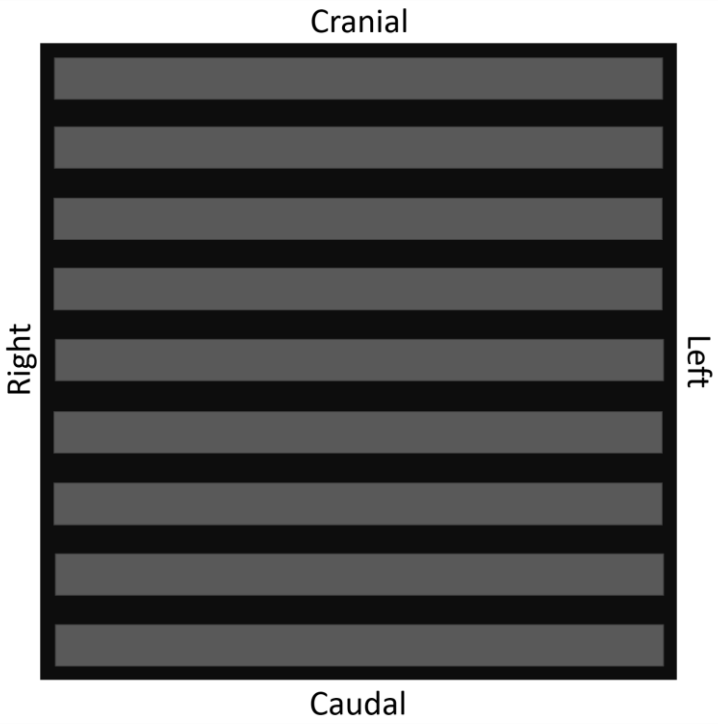

Source: the author

To obtain a map for comparison with the one generated by DM, each matrix was positioned between the examination table and a 19 cm-thick PMMA stack, following a geometry similar to that shown in Figure 1, which ensures that $d_{Ka,r}$ and d_{KPE} are identical. The setup was irradiated with a sequence of irradiation fields in different table positions, so the OSLDs were not uniformly exposed, and the resulting maps contained regions of overlap and varying irradiation field distributions.

The same experimental procedure was repeated, replacing the OSLD matrix with a Gafchromic® XR-RV3 radiochromic film, in order to obtain regions of dose distribution and field overlap.

After reading and processing the data from the OSLDs, the results were used to generate the dose maps, with the aim of comparing them to those generated by DM. To accomplish this, the Origin® software was used, employing a Heatmap plot.

2.4. Clinical Evaluation

To evaluate the dose mapping method of DM in a clinical context, the Percutaneous Transhepatic Biliary Drainage (PTBD) procedure was selected. It is one of the the most frequently performed procedure on the GE® Innova 4100 IQ angiography system, according to the institution's PACS system. It accounted for 17% of all procedures performed on this equipment between January 2023 and January 2024. This procedures is a liver intervention.

Each patient dose distribution was acquired with the OSLD matrix fixed on the examination table, at a position approximately in the liver region, positioned before the patient entered the room. Each matrix remained in the position throughout the entire procedure and was collected after the patient departure. Twelve patients from the IR sector of INRAD were evaluated, all undergoing the PTBD procedure. This study was approved by the Research Ethics Committee of HCFMUSP (CAAE 27912619.6.0000.0068), and informed consent was not required.

3. RESULTS AND DISCUSSIONS

3.1. OSLDs calibration

Figure 4 shows the graph of OSL signal versus air kerma, along with the linear fit to the experimental data (R^2=0.999): $C = 55.0K$, where C is the reading signal, in counts and K represents the kerma (mGy). The BG count, was subtracted from each reading before plotting.

Figure 4: Result of OSLDs calibration. The slope of the fitted line is 55.0±0.9 counts/mGy.

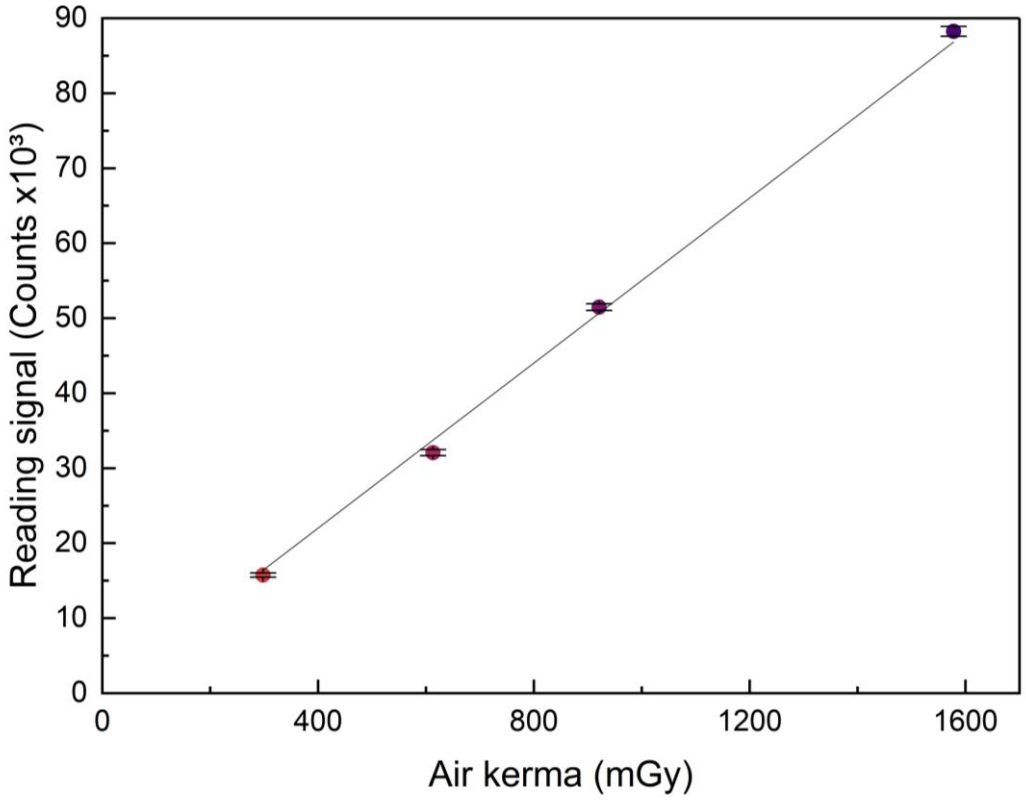

Source: the author

The calibration curve presented in Figure 4 showed the expected linear relationship between the OSL signal and air kerma [16]. The calibration factor $\left(\frac{1}{55.0}\right)$ obtained was consistently used throughout this study to convert OSL signal to air kerma wherever this transformation was required.

The calibration of the OSLDs was performed under a single beam condition, considering specific tube voltage and filtration parameters. OSLDs present energy dependence [17], and the use of these dosimeters under very different beam conditions may require either a new calibration or the determination of an energy correction factor.

Angiography systems typically operate with automatic exposure control (AEC) permanently enabled, meaning that the system automatically selects parameters such as tube voltage, filtration, and current based on beam attenuation. In this scenario, it is not possible

to manually control the irradiation parameters. To standardize the beam conditions for the measurements performed in this study, PMMA attenuators to simulate a patient were used at all stages, except on clinical evaluation.

3.2. Comparison of the $K_{a,r}$ from the Dose Map and OSLDs

Table 1 presents a comparison between the $K_{a,r}$ values provided by DM and the K_a obtained from the OSLDs. The $K_{a,r}$ values presented by the software, when compared to those measured by the OSLDs, show a maximum deviation of 14% in accuracy, as shown in Table 1. The $K_{a,r}$ is one of the parameters used in the dose map calculation presented by DM; therefore, based on the obtained results, it can be considered an appropriate input parameter for the dose map calculation performed by the software.

Table 1: Comparison of K_a values from OSLDs and $K_{a,r}$ from Dose Map.

K_a(mGy)	$K_{a,r}$(mGy)	Accuracy Deviation
177 ± 3	159 ± 28	10%
360 ± 6	330 ± 58	8%
578 ± 9	495 ± 87	14%
991 ± 16	1578 ± 149	14%

The observed result was expected, as national regulations stipulate a maximum of 20% for the accuracy deviation of $K_{a,r}$. Compliance with this requirement is ensured through annual testing and monitoring by the institution's medical physics team, as part of the quality control program.

3.3. Dose mapping with Phantoms

The maps produced are presented in Figure 5, along with DM corresponding picture, at the same grayscale. Figure 6 presents the comparison between a DM and the radiochromic film, scanned using an Epson Expression 10000 XL scanner. Dose calibration was not necessary in this case, as the goal was to perform a qualitative assessment.

Figure 5: Comparison results between the Dose Map (left) and the map constructed with the OSLDs matrix data (right) for the phantom tests. The yellow dashed lines represent the spatial comparison between the Dose Map and the map created with the OSLDs, and the "X" markings correspond to the grayscale tone indicated on their respective scale.

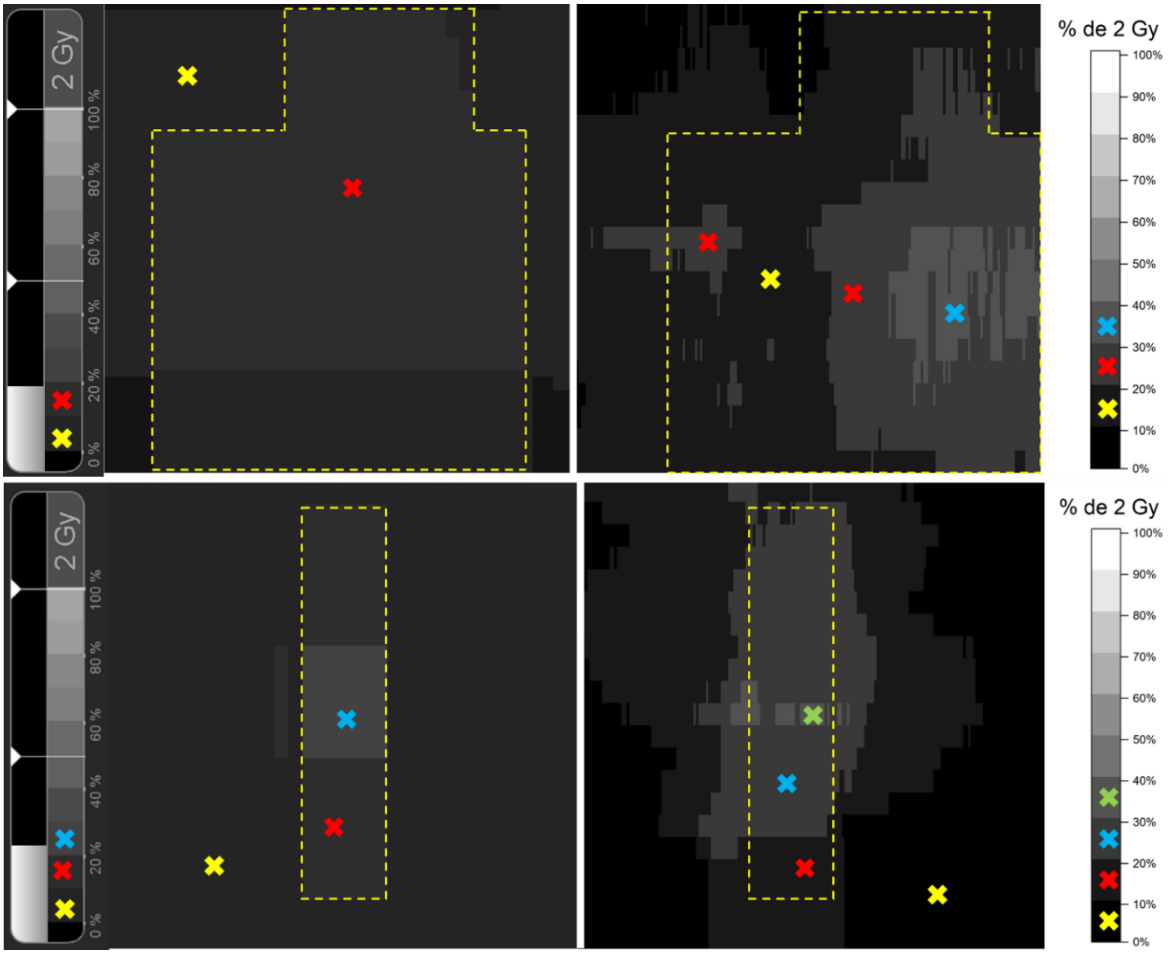

Source: the author

Figure 5 shows that there is a visual correspondence between the maps generated from the data of the OSLDs and DM method. The work by Bordier et al. (2014) [6] demonstrated that the uncertainty in the DM ESD calculation can range from 25% to 40%, considering the uncertainties in the components of Equation 2.

Additionally, the use of a radiochromic film confirmed that the maps generated by DM exhibit good geometric accuracy in qualitative comparisons. Furthermore, they accurately represent the overlaps of the irradiation fields, as illustrated in Figure 6.

Figure 6: Comparison results between the Dose Map (left) and the radiochromic film (right). The yellow dashed lines represent the spatial comparison between the Dose Map and the map obtained with the film, and the "X" markings correspond to equivalent regions identified by both methods.

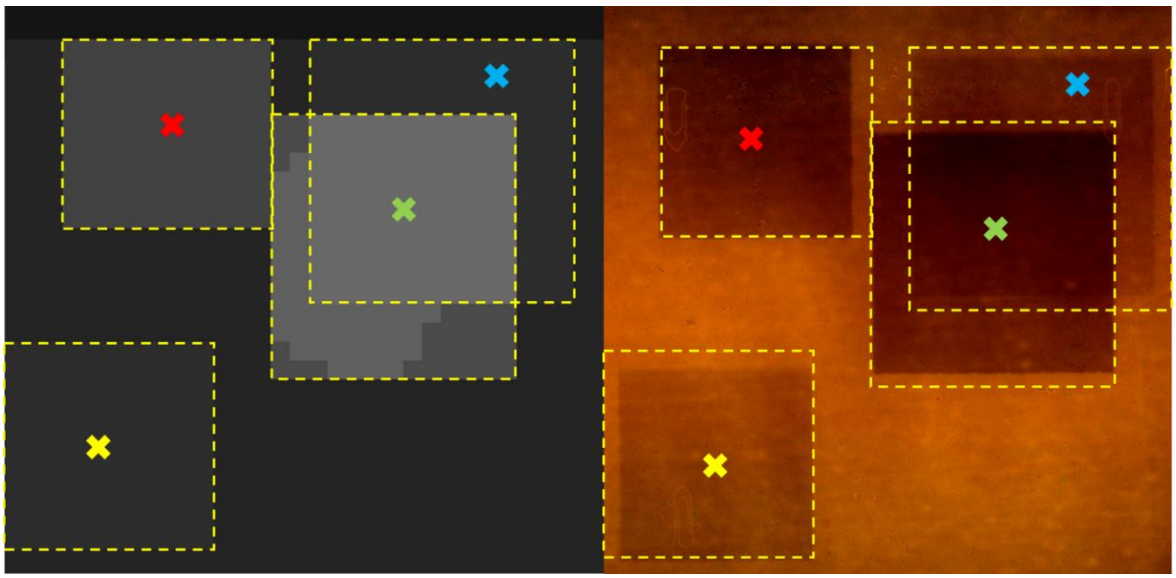

Source: the author

Despite all the potential sources of uncertainty associated with the Dose Map mapping method, one of its most beneficial applications is the ability to monitor the map in real-time during procedures. This allows the interventional physician to change the beam incidence region by adjusting the angulation of the C-arm or patient position, thus avoiding excessive dose absorption in a single skin region, which could lead to undesirable tissue reactions.

3.4. Clinical Evaluation

Following the same methodology described in subsection 3.3, OSLDs dose maps were generated for the patient monitoring procedures, as presented in Figure 7, with the corresponding DM results.

According to Figure 7, both maps demonstrated good visual agreement. However, to obtain the two comparable maps, data from twelve different patients were collected. The other ten cases could not be compared due to errors related to the positioning of the OSLD matrix on the table. Since the matrices do not cover a large area, there is a high likelihood that they may be outside the irradiated region.

Figure 7: Comparison results between the Dose Map (left) and the map constructed with the OSLD matrix data (right) for the monitoring of two different patients (upper and lower maps, respectively). The yellow dashed lines represent the spatial comparison between the Dose Map and the map created with the OSLDs, and the "X" markings correspond to the grayscale tone indicated on their respective scale.

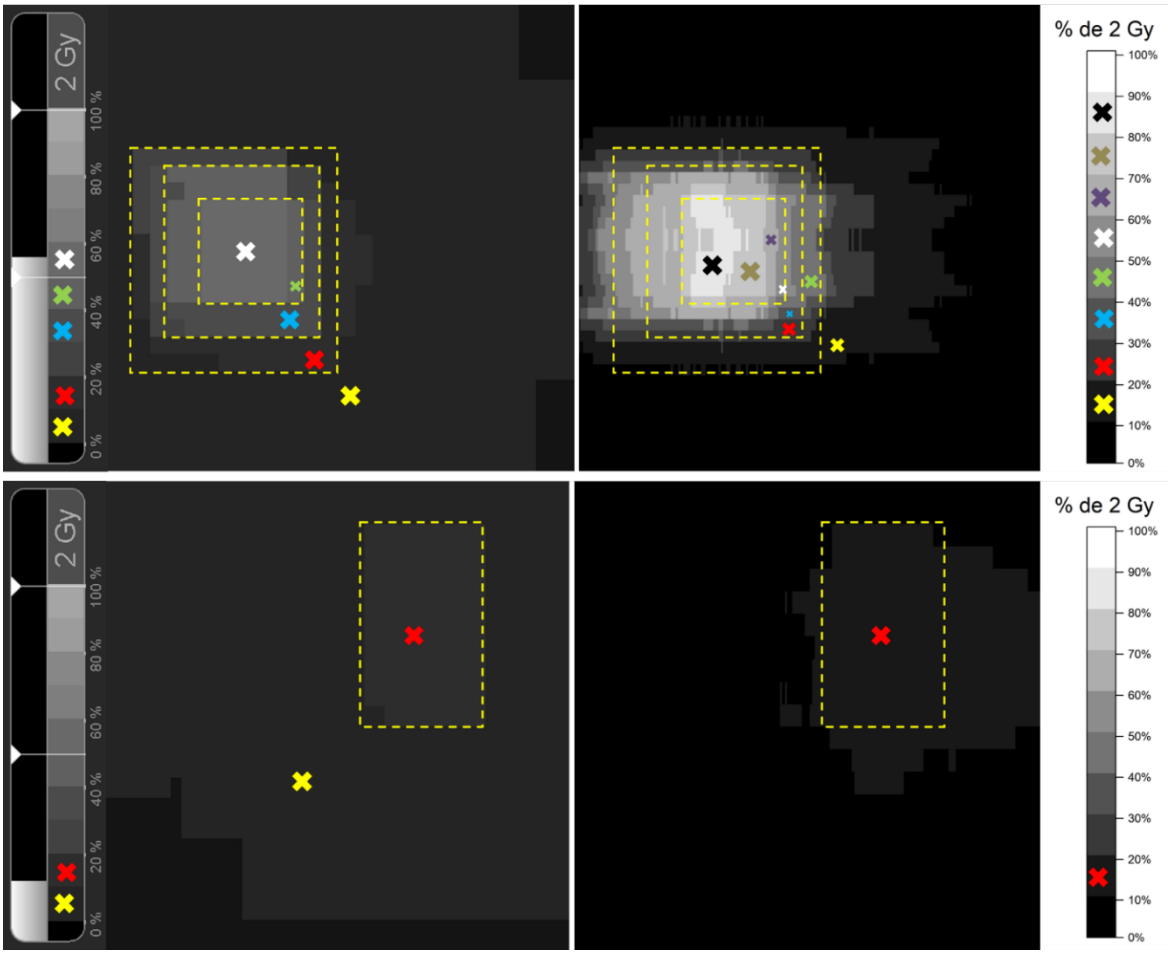

Source: the author

Additionally, for the results presented in subsection 3.3, both the OSLDs and the radiochromic film were used under controlled beam, attenuation, and scattering conditions. Both OSLDs and radiochromic films exhibit energy dependence [6, 17]. In clinical settings, however, the irradiations are not performed under a controlled setting and may present variations in energy and filtration between exposures, due to the use of AEC system. This represents a limiting factor in the clinical use of these types of dosimetry, as the energy dependence may lead to greater discrepancies between the measured and actual dose values.

This highlights the importance of automatic dose assessment methods such as DM, which have already been demonstrated in this and other studies [6, 18, 19] good agreement

between the irradiated areas and the regions of field overlap. Moreover, it is recommended to evaluate the consistency of dose mapping methods during the acceptance testing of equipment supplied with this type of software [20]. Additionally, it is advisable to re-evaluate the method in cases of repairs or replacement of components that may affect the mapping process.

4. CONCLUSIONS

The results of this study demonstrated the effectiveness of DM in assessing ESD distribution during IR procedures. The comparison between the maps generated by DM, those obtained using OSLDs matrices and radiochromic films indicated good geometric accuracy and a reliable representation of irradiation field overlaps. Furthermore, the $K_{a,r}$ values showed acceptable accuracy deviation between the values presented by the software and those measured with the dosimeters.

Despite the limitations related to the energy dependence of OSLDs and the complexity of measurements under clinical conditions, the dose maps obtained were consistent with those provided by the software. Additionally, the real-time monitoring capability offered by DM stands out as an important tool for optimizing radiation exposure, contributing to patient safety and dose control during procedures.

ACKNOWLEDGMENT

The author would like to thank Faculdade de Medicina da Universidade de São Paulo (FMUSP) for the residency opportunity. Special thanks to Nancy Umisedo for her assistance with the POSLI reader, and to Renan Ikeda for providing the Python code used in data analysis.

FUNDING

This study was conducted as the final project of the Medical Physics Residency Program in Diagnostic Imaging at FMUSP, funded by a scholarship from the Brazilian Ministry of Health's National Residency Program in Health Professions. EMY is funded by CNPq and FAPESP (grants: 311657/2021-4, and 2018/05982-0, respectively).

CONFLICT OF INTEREST

All authors declare that they have no conflicts of interest.

DATA AVAILABILITY STATEMENT

The authors declare that the data supporting the results of this study are available in the article. Derived data supporting the conclusions of this study are available upon request from the corresponding author.

REFERENCES

[1] O'BRIEN, B.; VAN DER PUTTEN, W. Quantification of risk-benefit in interventional radiology. **Radiation protection dosimetry**, v. 129, n. 1-3, p. 59–62, 2008. DOI: <https://doi.org/10.1093/rpd/ncn040>.

[2] WAGNER, L. K.; EIFEL, P. J.; GEISE, R. A. Potential biological effects following high X-ray dose interventional procedures. **Journal of Vascular and Interventional Radiology**, v. 5, n. 1, p. 71–84, 1994. DOI: <https://doi.org/10.1016/S1051-0443(94)71456-1>.

[3] JASCHKE, W. et al. Radiation-induced skin injuries to patients: what the interventional radiologist needs to know. **CardioVascular and Interventional Radiology**, v. 40, n. 8, p. 1131–1140, 2017.

[4] International Electrotechnical Commission. Medical electrical equipment, part 2-43 - particular requirements for the safety of X-ray equipment for interventional procedures. IEC 60601-2-43, 2000.

[5] Digital Imaging and Communications in Medicine (DICOM). Supplement 94: diagnostic X-ray radiation dose reporting (Dose SR). 2005.

[6] BORDIER, C.; KLAUSZ, R.; DESPONDS, L. Patient dose map indications on interventional X-ray systems and validation with Gafchromic™ XR-RV3 film. **Radiation protection dosimetry**, v. 163, n. 3, p. 306–318, 2015. DOI: <https://doi.org/10.1093/rpd/ncu181>.

[7] KUMAR, D.; PRADHAN, A.; CHAUHAN, V. Utilizing Gafchromic™ EBT3 film for precise skin dosimetry in head and neck cancer patients. **Journal of Radioanalytical and Nuclear Chemistry**, p. 1–10, 2024.

[8] AKDENIZ, Y. Comparative analysis of dosimetric uncertainty using Gafchromic™ EBT4 and EBT3 films in radiochromic film dosimetry. **Radiation Physics and Chemistry**, v. 220, p. 111723, 2024. DOI: <https://doi.org/10.1016/j.radphyschem.2024.111723>.

[9] LIN, Y.-F. et al. In vivo dosimetry using EBT3 and EBT-XD radiochromic films for high-energy electron beam in hypofractionation keloid radiotherapy. **Radiation Physics and Chemistry**, v. 218, p. 111575, 2024. DOI: <https://doi.org/10.1016/j.radphyschem.2024.111575>.

[10] HADID-BEURRIER, L. et al. Clinical benchmarking of a commercial software for skin dose estimation in cardiac, abdominal, and neurology interventional procedures. **Medical Physics**, v. 51, n. 5, p. 3687–3697, 2024. DOI: <https://doi.org/10.1002/mp.16956>.

[11] CANNE, S. D. et al. Use of Gafchromic™ XR type R films for skin-dose measurements in interventional radiology: Validation of a dosimetric procedure on a sample of patients undergone interventional cardiology. **Physica Medica**, v. 22, n. 3, p. 105–110, 2006. DOI: <https://doi.org/10.1016/S1120-1797(06)80004-9>.

[12] KIDOŃ, J. et al. Calibration of Gafchromic™ XR-RV3 film under interventional radiology conditions. **Polish Journal of Medical Physics and Engineering**, v. 27, n. 2, p. 165–173, 2021. DOI: <https://doi.org/10.2478/pjmpe-2021-0020>.

[13] YUKIHARA, E. G.; MCKEEVER, S. W. S. Optically stimulated luminescence (OSL) dosimetry in medicine. **Physics in Medicine & Biology**, v. 53, n. 20, p. R351, 2008. DOI: <https://doi.org/10.1088/0031-9155/53/20/R01>

[14] UMISEDO, N. K.; YOSHIMURA, E. M. POSLI–instrumentação para leitura de detetores OSL em forma de fita. In: **ANAIS XXII CBFM 2017**. Ribeirão Preto, São Paulo: [s.n.], 2017. Disponível em: <https://www.cbfm.net.br/2017>.

[15] International Atomic Energy Agency (IAEA). Dosimetry in Diagnostic Radiology: An International Code of Practice. Viena, Áustria, 2007. Disponível em: <https://www-pub.iaea.org/MTCD/Publications/PDF/TRS457_web.pdf>.

[16] TAKEGAMI, K. et al. Practical calibration curve of small-type optically stimulated luminescence (OSL) dosimeter for evaluation of entrance skin dose in the diagnostic X-ray region. **Radiological Physics and Technology**, v. 8, p. 286–294, 2015.

[17] AL-SENAN, R. M.; HATAB, M. R. Characteristics of an OSLD in the diagnostic energy range. **Medical physics**, v. 38, n. 7, p. 4396–4405, 2011. DOI: <https://doi.org/10.1118/1.3602456>.

[18] BORDIER, C.; KLAUSZ, R.; DESPONDS, L. Accuracy of a dose map method assessed in clinical and anthropomorphic phantom situations using Gafchromic™ films. **Radiation protection dosimetry**, v. 165, n. 1-4, p. 244–249, 2015. DOI: <https://doi.org/10.1093/rpd/ncv034>.

[19] DIDIER, R. et al. In vivo validation of Dosemap software use in interventional cardiology with dosimetrics indicators and peak skin dose evaluation. **Catheterization and Cardiovascular Interventions**, v. 94, n. 2, p. 216–222, 2019. DOI: <https://doi.org/10.1002/ccd.28097>.

[20] European Federation of Organisations for Medical Physics (EFOMP). Quality control of dynamic X-ray imaging systems. 2024. Disponível em: <https://abrir.link/uWEeY>.

LICENSE